Reprinted from JOURNAL OF COMPUTATIONAL PHYSICS

Vol. 108, No. 1, September 1993
Printed in Belgium

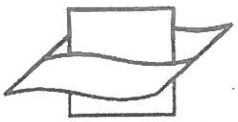

Stability of a FBTCS Scheme Applied to the Propagation of Shallow-Water Inertia-Gravity Waves on Various Space Grids

JEAN-MARIE BECKERS

GHER, Sart Tilman, B5, University of Liège, B-4000 Liège, Belgium

AND

ERIC DELEERSNIJDER

G. Lemaitre Institute of Astronomy and Geophysics, Chemin du Cyclotron 2, Catholic University of Louvain, B-1348 Louvain-la-Neuve, Belgium

Received June 17, 1991; revised November 5, 1992

The equations governing the propagation of inertia-gravity waves in geophysical fluid flows are discretized on the A, B, C, and D grids according to the classical forward–backward on time and centered on space (FBTCS) numerical scheme. The von Neumann stability analysis is performed and it is shown that the stability condition of the inertia-gravity waves scheme is more restrictive, at least by a factor of $\sqrt{2}$, than that concerning pure gravity waves, whatever the magnitude of the Coriolis parameter. Finally, the general necessary and sufficient stability condition is derived for the A, B and C grids, while, on the D grid, the stability condition has been obtained only in particular cases.

1. INTRODUCTION

Large scale atmospheric and oceanic motions roughly obey the geostrophic equilibrium. When imbalances occur, the geostrophic balance is restored by means of inertia-gravity waves (Rossby [14, 15]; Cahn [5]; Obukhov [13]; Washington [22]; Blumen [4]; Schoenstadt [17]; Hsieh and Gill [7]). The dynamics of tides and storm surges are dominated by the propagation of external inertia-gravity waves, which are related to the motion of the sea surface. In strongly stratified seas, one also considers the displacement of density surfaces, which leads to internal inertia-gravity waves. The propagation of inertia-gravity waves, be they external or internal, is thus a central issue to many geophysical fluid models. Hence, it is of highest importance that the numerical scheme utilized be able to properly represent the propagation of those waves.

The external linear inertia-gravity waves, also called Poincaré waves, are governed by the following dimensionless equations,

$$\frac{\partial \eta}{\partial t}+\frac{\partial u}{\partial x}+\frac{\partial v}{\partial y}=0, \tag{1}$$

$$\frac{\partial u}{\partial t}-fv=-\frac{\partial \eta}{\partial x}, \tag{2}$$

$$\frac{\partial v}{\partial t}+fu=-\frac{\partial \eta}{\partial y}, \tag{3}$$

where t is the time, u and v are horizontal velocity components in the x and y direction, respectively, and η is the sea surface elevation. The characteristic length, L, and time, T, used in the derivation of the dimensionless variables obey

$$L^2=ghT^2, \tag{4}$$

where g is the gravitational acceleration and h is the unperturbed depth of the sea, supposed to be constant. The velocity scale, U, and the elevation scale, E, satisfy

$$E^2=\frac{hU^2}{g}. \tag{5}$$

In addition, $\tilde{f}$ being the Coriolis parameter, f is defined to be

$$f=\tilde{f}T \tag{6}$$

so that the pure gravity waves correspond to $f=0$.

The governing equations of internal inertia-gravity waves are similar to (1)–(3), except that h, u, v, and η are to be interpreted as equivalent quantities related to the particular internal mode considered (LeBlond and Mysak [10]).

Various discretized forms of (1)–(3) have been examined (Winninghoff [23]; Schoenstadt and Williams [16]; Arakawa and Lamb [1]; Schoenstadt [17]; Schoenstadt [18]; Batteen and Han [2]). Those studies focus on the space differencing aspects. When time differencing is also

0021-9991/93 $5.00

considered, it is customary to restrict the analysis to pure gravity waves ($f = 0$). In this case, the stability conditions of the numerical scheme are readily obtained.

In the present article, on the example of a simple time-space differencing scheme, we show that the stability condition of the scheme representing the propagation of inertia-gravity waves is far more constraining than that of the pure gravity waves scheme. Indeed, the limit as $f \to 0$ of the stability conditions is not equal to the stability condition when $f = 0$.

It is worth pointing out that only very few authors have drawn attention to similar numerical problems. One may, however, mention Kasahara [9], Thacker [20, 21], Cushman-Roisin [6], or Beckers [3]. Interestingly enough, Thacker [20, 21] found a finite element scheme conditionally stable for pure gravity waves and unconditionally unstable whenever the Coriolis force is introduced.

2. THE FBTCS NUMERICAL SCHEME

Winninghoff [23] has shown that the numerical propagation of Poincaré waves strongly depends on the distribution of u, v, and η over the grid points. Here, four types of numerical lattices are studied, namely the A, B, C, and D grids, according to Arakawa's classification (Arakawa and Lamb [1]) (Fig. 1). Using the following notations,

$$a_{n_t, n_x, n_y} = a(t = n_t\,\Delta t,\ x = n_x\,\Delta x,\ y = n_y\,\Delta y), \tag{7}$$

$$(\delta_x a)_{n_x} = \{a[(n_x + \tfrac{1}{2})\,\Delta x] - a[(n_x - \tfrac{1}{2})\,\Delta x]\}/\Delta x, \tag{8}$$

$$(\bar{a}^x)_{n_x} = \{a[(n_x + \tfrac{1}{2})\,\Delta x] + a[(n_x - \tfrac{1}{2})\,\Delta x]\}/2, \tag{9}$$

the FBTCS scheme reads

A-grid,

$$\begin{aligned}
&(\delta_t \eta)_{n_t + 1/2, n_x, n_y} + (\delta_x \bar{u}^x)_{n_t, n_x, n_y} + (\delta_y \bar{v}^y)_{n_t, n_x, n_y} = 0\\
&(\delta_t u)_{n_t + 1/2, n_x, n_y} - f v_{n_t + s, n_x, n_y}\\
&\qquad = -(\delta_x \bar{\eta}^x)_{n_t + 1, n_x, n_y}\\
&(\delta_t v)_{n_t + 1/2, n_x, n_y} + f u_{n_t + 1 - s, n_x, n_y}\\
&\qquad = -(\delta_y \bar{\eta}^y)_{n_t + 1, n_x, n_y};
\end{aligned} \tag{10}$$

B-grid,

$$\begin{aligned}
&(\delta_t \eta)_{n_t + 1/2, n_x, n_y} + (\delta_x \bar{u}^y)_{n_t, n_x, n_y} + (\delta_y \bar{v}^x)_{n_t, n_x, n_y} = 0\\
&(\delta_t u)_{n_t + 1/2, n_x + 1/2, n_y + 1/2} - f v_{n_t + s, n_x + 1/2, n_y + 1/2}\\
&\qquad = -(\delta_x \bar{\eta}^y)_{n_t + 1, n_x + 1/2, n_y + 1/2}\\
&(\delta_t v)_{n_t + 1/2, n_x + 1/2, n_y + 1/2} + f u_{n_t + 1 - s, n_x + 1/2, n_y + 1/2}\\
&\qquad = -(\delta_y \bar{\eta}^x)_{n_t + 1, n_x + 1/2, n_y + 1/2};
\end{aligned} \tag{11}$$

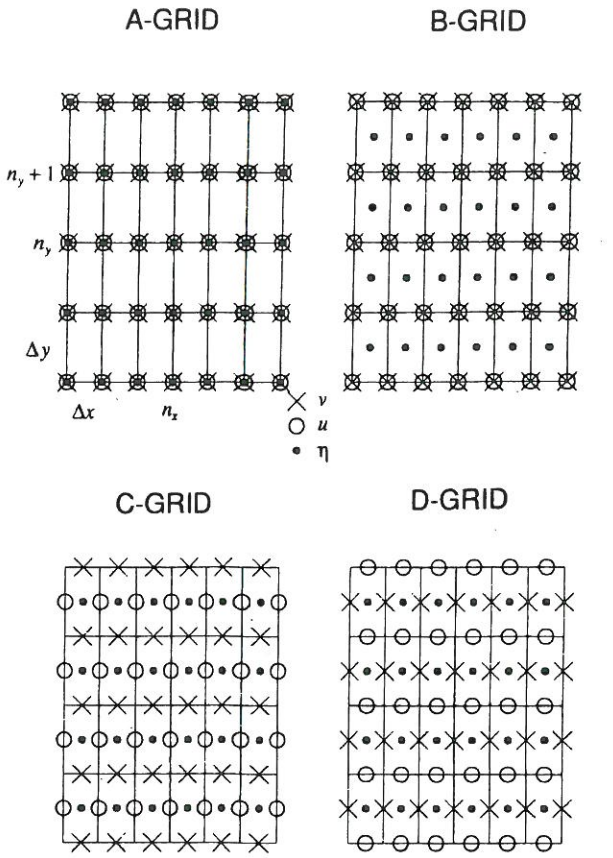

FIG. 1. Spatial distribution of the variables (η, u, v) on the A, B, C, and D grids. The space density of the discrete variables is equal on all of the grids.

C-grid,

$$\begin{aligned}
&(\delta_t \eta)_{n_t + 1/2, n_x, n_y} + (\delta_x u)_{n_t, n_x, n_y} + (\delta_y v)_{n_t, n_x, n_y} = 0\\
&(\delta_t u)_{n_t + 1/2, n_x + 1/2, n_y} - f \bar{v}^{xy}_{n_t + s, n_x + 1/2, n_y}\\
&\qquad = -(\delta_x \eta)_{n_t + 1, n_x + 1/2, n_y}\\
&(\delta_t v)_{n_t + 1/2, n_x, n_y + 1/2} + f \bar{u}^{xy}_{n_t + 1 - s, n_x, n_y + 1/2}\\
&\qquad = -(\delta_y \eta)_{n_t + 1, n_x, n_y + 1/2};
\end{aligned} \tag{12}$$

D-grid

$$\begin{aligned}
&(\delta_t \eta)_{n_t + 1/2, n_x, n_y} + (\delta_x \bar{u}^{xy})_{n_t, n_x, n_y} + (\delta_y \bar{v}^{xy})_{n_t, n_x, n_y} = 0\\
&(\delta_t u)_{n_t + 1/2, n_x, n_y + 1/2} - f \bar{v}^{xy}_{n_t + s, n_x, n_y + 1/2}\\
&\qquad = -(\delta_x \bar{\eta}^{xy})_{n_t + 1, n_x, n_y + 1/2}\\
&(\delta_t v)_{n_t + 1/2, n_x + 1/2, n_y} + f \bar{u}^{xy}_{n_t + 1 - s, n_x + 1/2, n_y}\\
&\qquad = -(\delta_y \bar{\eta}^{xy})_{n_t + 1, n_x + 1/2, n_y};
\end{aligned} \tag{13}$$

where s is zero or one according to whether n_t is even or odd.

The centered space differencing in (10)–(13) is equivalent to that of Arakawa and Lamb [1], while the time stepping of the gravity wave part is similar to the forward–backward scheme (Mesinger and Arakawa [12]). One prevents the Coriolis force from generating mechanical power by a simple technique stemming from Sielecki [19] and adapting it to ensure symmetry in the x and y directions. The discretized time derivatives may be regarded as forward or backward, depending on the term one is considering. The name FBTCS is therefore suggested for the above schemes: forward-backward on time and centered on space.

The von Neumann stability analysis is now applied to the discretized equations (10)–(13). First, one defines a spatially periodic solution

$$\begin{pmatrix}\eta\\ u\\ v\end{pmatrix}=\begin{pmatrix}\mathscr{E}(t)\\ \mathscr{U}(t)\\ \mathscr{V}(t)\end{pmatrix}e^{i(k_x x+k_y y)}=\mathbf{x}_{n_t}e^{i(n_x 2\theta_x+n_y 2\theta_y)}, \tag{14}$$

where θ_x and θ_y are related to the wavenumbers k_x and k_y by $0\leqslant 2\theta_x=k_x\,\Delta x\leqslant\pi$ and $0\leqslant 2\theta_y=k_y\,\Delta y\leqslant\pi$. Next, this periodic solution (14) is introduced into the discretized equations (10)–(13), leading for each grid to the expression

$$A_s\mathbf{x}_{n_t+1}+B_s\mathbf{x}_{n_t}=0,\qquad s=0,\ 1. \tag{15}$$

Since the time discretization of the Coriolis terms varies according to the value of s, the amplification matrix of the scheme must be built over two time steps. For the A, B, C, and D grids, one then obtains

$$\mathbf{x}_{2n_t}=(A_1^{-1}B_1A_0^{-1}B_0)^{n_t}\mathbf{x}_0 \tag{16}$$

and

$$\mathbf{x}_{2n_t+1}=(A_0^{-1}B_0A_1^{-1}B_1)^{n_t}\mathbf{x}_1. \tag{17}$$

Finally, one may thus define two amplification matrices:

$$H_{10}=A_1^{-1}B_1A_0^{-1}B_0, \tag{18}$$

$$H_{01}=A_0^{-1}B_0A_1^{-1}B_1. \tag{19}$$

Calculating the elements of H_{10} and H_{01} is, in principle, straightforward. However, it turns out to demand lengthy algebraic manipulations, which we performed by means of a symbolic computations software.

It must be pointed out that H_{10} and H_{01}, although non-equal, have the same eigenvalues, hereafter denoted ρ. As the time-independent geostrophic motion is a possible solution to (10)–(13), one eigenvalue will be unity. In fact, for each grid, the characteristic equation of either H_{10} or H_{01} may be factorized as

$$(\rho-1)(-\rho^2+2b\rho-1)=0. \tag{20}$$

Equations (1)–(3) contain no phenomena growing in time. This implies that the von Neumann stability condition is

$$|\rho|\leqslant 1 \tag{21}$$

or, equivalently,

$$-1\leqslant b\leqslant 1. \tag{22}$$

Upon defining

$$\phi=f\,\Delta t, \tag{23}$$

$$(c_x,\,c_y)=\left(\frac{\Delta t}{\Delta x},\,\frac{\Delta t}{\Delta y}\right), \tag{24}$$

and

$$\xi=\xi_x+\xi_y\qquad(\xi_x,\,\xi_y\geqslant 0), \tag{25}$$

b reads

$$b=1-8\,\frac{(\xi_*-\xi)\xi}{\xi_*^2}-2\phi^2\alpha^2\left[4\,\frac{\xi_x\xi_y}{\xi_*^2}+\frac{(\xi_*-2\xi)}{\xi_*}\right], \tag{26}$$

where α, ξ_*, ξ_x, and ξ_y are given in Table I.

We now have to find the constraints on ϕ, c_x, and c_y that ensure (22).

TABLE I

Definition of α, ξ_*, ξ_x, and ξ_y for grids A, B, C, and D

Grid	α	ξ_*	ξ_x/c_x^2	ξ_y/c_y^2
A	1	4	$\sin^2 2\theta_x$	$\sin^2 2\theta_y$
B	1	1	$\sin^2\theta_x\cos^2\theta_y$	$\sin^2\theta_y\cos^2\theta_x$
C	$\lvert\cos\theta_x\cos\theta_y\rvert$	1	$\sin^2\theta_x$	$\sin^2\theta_y$
D	$\lvert\cos\theta_x\cos\theta_y\rvert$	1	$\alpha^2\sin^2\theta_x$	$\alpha^2\sin^2\theta_y$

3. SIMPLE NECESSARY STABILITY CONDITIONS

Pure inertia oscillations correspond to infinitely long waves, $\theta_x=\theta_y=0$. In this case, the space derivatives vanish and we obviously find the same stability condition for all of the grids:

$$\phi^2\leqslant 1. \tag{27}$$

Putting $\phi=0$ yields the classical pure gravity waves problem, widely analysed for a large variety of schemes, including ours (e.g., Janjic [8], Schoenstadt and Williams

TABLE II

Summary of the von Neumann Stability Conditions Establishes in the Present Article

Grid	Inertia oscillations	Pure gravity waves		Inertia-gravity waves	
		$c_x = c = c_y$	$c_x \neq c_y$	$c_x = c = c_y$	$c_x \neq c_y$
A	$\phi^2 \leqslant 1$	$c^2 \leqslant 2$	$c_x^2 + c_y^2 \leqslant 4$	$c^2 \leqslant 2\dfrac{2 - \lvert\phi\rvert - \phi^2}{4 - \phi^2}$	$c_x^2 + c_y^2 \leqslant \dfrac{2 - \phi^2 - \lvert\phi\rvert\sqrt{\phi^2 + (1-\phi^2)\sin^2 2\beta}}{1 - \phi^2 \sin^2\beta\cos^2\beta}$ where $\sin^2\beta = \dfrac{c_y^2}{c_x^2 + c_y^2}$
B	$\phi^2 \leqslant 1$	$c^2 \leqslant 1$	$c_x^2, c_y^2 \leqslant 1$	$c^2 \leqslant \dfrac{1-\phi^2}{2}$	$c_x^2, c_y^2 \leqslant \dfrac{1-\phi^2}{2}$
C	$\phi^2 \leqslant 1$	$c^2 \leqslant \frac{1}{2}$	$c_x^2 + c_y^2 \leqslant 1$	$\phi^2 \leqslant 1$ and $c^2 \leqslant \frac{1}{4}$	$\phi^2 \leqslant 1$ and $c_x^2 + c_y^2 \leqslant \frac{1}{2}$
D	$\phi^2 \leqslant 1$	$c^2 \leqslant \frac{27}{8}$	$c_x^2, c_y^2 \leqslant 4$ and $\dfrac{(c_x^2 + c_y^2)^3}{27 c_x^2 c_y^2} \leqslant 1$ if $c_x^2 + c_y^2 \geqslant 6$	$c^2 \leqslant \dfrac{1}{2}\min\limits_{0 \leqslant \alpha \leqslant 1}\left[\dfrac{1 - \alpha\lvert\phi\rvert}{\alpha^2(1-\alpha)(2-\alpha\lvert\phi\rvert)}\right]$	Unknown in general $c_x^2, c_y^2 \leqslant \frac{1}{2}$ if $\phi^2 = 1$ $c_x^2 \leqslant \frac{1}{2}(1 + \sqrt{1-\phi^2})^2$ if $c_y = 0$

Note. All conditions are necessary and sufficient. However, criteria for pure inertia oscillations and pure gravity waves may be considered necessary conditions for the inertia-gravity waves problem. The $\phi^2 \leqslant 1$ condition is implicitly contained in all of the conditions of the rightmost two columns, except those of the C grid.

[16], Mesinger [11], Mesinger and Arakawa [12]). In this case, condition (22) immediately leads to the necessary and sufficient stability condition

$$\xi \leqslant \xi_*, \tag{28}$$

which is easily translated into constraints on c_x and c_y in Table II. Only the lesser known D-grid stability analysis is given in Appendix I.

When neither ϕ nor θ_x nor θ_y are zero, it is clear that for $\xi \to \xi_*/2$ one has

$$b = -1 - 8\alpha^2\phi^2\frac{\xi_x\xi_y}{\xi_*^2}. \tag{29}$$

Numerical stability of inertia-gravity waves schemes thus necessitates

$$\xi \leqslant \xi_*/2, \tag{30}$$

which means that the maximum admissible time step is, **at most**, equal to that of pure gravity waves divided by a factor of $\sqrt{2}$. This holds true whatever the value of f, provided $f \neq 0$!

Inequalities (27) and (30) are thus necessary stability conditions for the Poincaré waves scheme.

4. GRAPHICAL INTERPRETATION

According to Eq. (26), b is a quadratic function of ξ_x and ξ_y. The fact that the stability constraint for $\phi = 0$ is different from that found for $\phi^2 \to 0$ stems from a singular perturbation problem that arises because ϕ^2 is a multiplicative factor of $\xi_x\xi_y$, which is one of the highest degree terms of (26). A graphical interpretation, however, turns out to be more striking and also proves to be a helpful guide line in the determination of the necessary and sufficient stability conditions.

Given a fixed value of b and α, (ξ_x, ξ_y) describes an elliptical path in the ξ_x, ξ_y-space. By varying b, one obtains concentric ellipses whose axes grow as b increases. Indeed, the ellipse center is located at

$$(\xi_{x,c}, \xi_{y,c}) = \frac{\xi_*(2 - \alpha^2\phi^2)}{2(4 - \alpha^2\phi^2)}(1, 1). \tag{31}$$

The minor axis,

$$e = \frac{\xi_*}{2(4 - \alpha^2\phi^2)}\sqrt{8(1+b) + 2(1-b)\alpha^2\phi^2}, \tag{32}$$

lies on the symmetry axis $\xi_x = \xi_y$. The existence of this symmetry axis will be the underlying basis of much of the

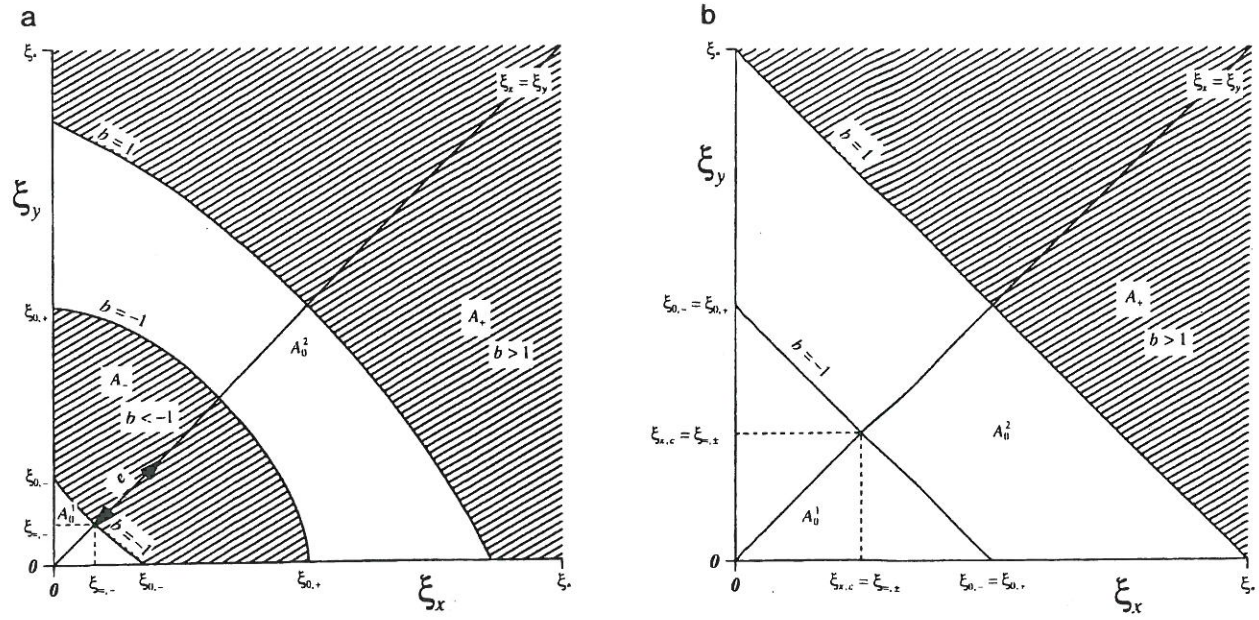

FIG. 2. Stability and instability (hatched) regions for $0 < \phi^2 \leqslant 1$ (a) and $\phi = 0$ (b).

following discussion. Intersections of the $b = -1$ ellipse with $\xi_y = 0$ and with symmetry line $\xi_x = \xi_y$ are, respectively, at

$$\xi_{0,\pm} = \frac{\xi_*}{4}\,[2 + \alpha^2\phi^2(-1 \pm 1)], \tag{33}$$

$$\xi_{*,\pm} = \frac{\xi_*(1 \pm \alpha\,|\phi|)}{2(2 \pm \alpha\,|\phi|)}. \tag{34}$$

The above ellipse features are illustrated in Fig. 2a.

According to the stability criterion (22), the subspace $\xi_x, \xi_y \geqslant 0$ is divided into three areas, $A_-, A_0 = A_0^1 \cup A_0^2$, and A_+, corresponding to $b < -1, -1 \leqslant b \leqslant 1$, and $1 < b$ (Fig. 2a). The stability conditions must be such that (ξ_x, ξ_y) always lies in A_0. Since ξ_x, ξ_y may vary—not necessarily independently—from 0 to c_x^2, c_y^2, respectively, it is clear that (ξ_x, ξ_y) cannot come into A_0^2 without crossing A_-. Hence, the actual stability constraint must force (ξ_x, ξ_y) to remain within A_0^1. When $\phi = 0$, the characteristic values (Eq. (32), (33), and (34)) of the $b = -1$ ellipse indicate that this ellipse transforms to a straight line so that A_- vanishes, which implies that the stability area is then A_0, instead of A_0^1 only (Fig. 2b). This "jump" of the stability line explains easily the fact that the stability condition changes with a discontinuity when $f = 0$ or $f \neq 0$. The factor $\sqrt{2}$ is also readily understood.

5. NECESSARY AND SUFFICIENT STABILITY CONDITIONS

The stability constraints derived below are collected in the two rightmost columns of Table II.

5.1. *A-Grid*

Let

$$(c_x, c_y) = c(\cos\beta, \sin\beta), \qquad 0 \leqslant \beta \leqslant \pi/2, \tag{35}$$

In Table I, it can be seen that ξ_x and ξ_y may vary independently, so that $c^2 = \max_{\theta_x, \theta_y}(\xi_x + \xi_y)$. As explained in Section 4, numerical stability requires that point (ξ_x, ξ_y) remains in the A_0^1 area, which means that (ξ_x, ξ_y) must be "beneath" the curve corresponding to $b = -1$ (see Fig. 3). This may be expressed as

$$c^2 \leqslant [c^2]_{b=-1}. \tag{36}$$

Introducing (35) into (26) with $b = -1$, (36) gives

$$c^2 \leqslant \frac{2 - \phi^2 - |\phi|\sqrt{\phi^2 + (1 - \phi^2)\sin^2 2\beta}}{1 - \phi^2 \sin^2\beta \cos^2\beta}. \tag{37}$$

5.2. *B-Grid*

In this case, ξ_x and ξ_y are both functions of θ_x and θ_y. According to Table I, the expressions defining ξ_x and ξ_y combine to give

$$\frac{\xi_y}{c_y^2} = \left(1 - \frac{1}{\sin^2\theta_x}\frac{\xi_x}{c_x^2}\right)(1 - \sin^2\theta_x), \tag{38}$$

which can be viewed as a family of segments of a line having their ends on the ξ_x and ξ_y axes and depending on the

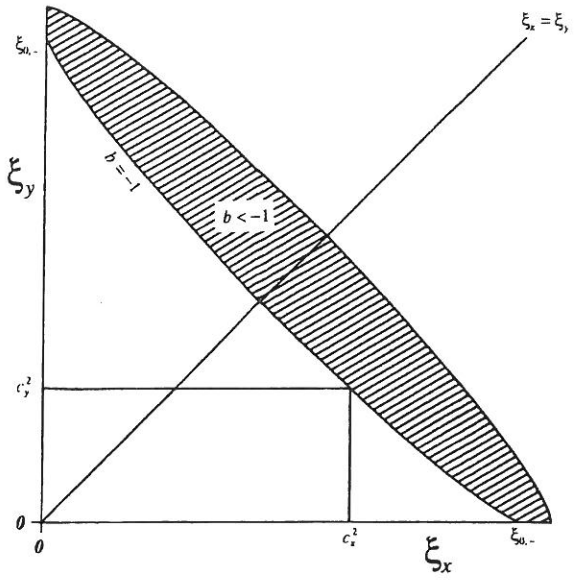

FIG. 3. Stability condition for grid A.

parameter $\sin^2 \theta_x$. The envelope curve is readily determined to be

$$\frac{\sqrt{\xi_x}}{c_x} + \frac{\sqrt{\xi_y}}{c_y} = 1. \tag{39}$$

Numerical stability simply requires that the envelope curve (39) lie in A_0^1 (Fig. 4). Examining the intersections of

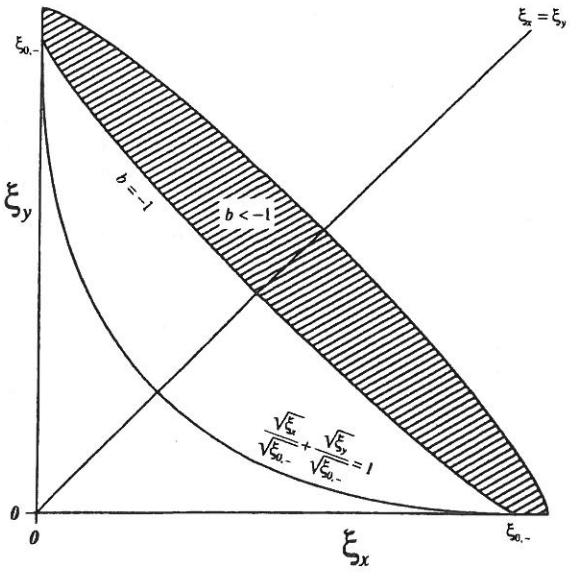

FIG. 4. Stability condition for grid B.

(39) with the ξ_x and ξ_y axes, leads to a necessary stability condition,

$$c_x^2,\ c_y^2 \leqslant \xi_{0,-} = \frac{1-\phi^2}{2}. \tag{40}$$

Since the envelope curve (39) always lies "beneath" the curve

$$\frac{\sqrt{\xi_x}}{\max(c_x)} + \frac{\sqrt{\xi_y}}{\max(c_y)} = 1, \tag{41}$$

it follows that (40) is also a sufficient stability condition because

$$\frac{\sqrt{\xi_x}}{\sqrt{\xi_{0,-}}} + \frac{\sqrt{\xi_y}}{\sqrt{\xi_{0,-}}} = 1 \tag{42}$$

does not enter the A_- region. This is readily demonstrated.

5.3. *C-Grid*

Here, the features of the ellipses are functions of (θ_x, θ_y) through α (Table I). When $\alpha \to 0$, (31)–(34) show that the $b = -1$ ellipse transforms to the segment of a line

$$\xi_x + \xi_y = \xi = \tfrac{1}{2}, \tag{43}$$

which immediately gives rise to the following necessary stability condition:

$$c_x^2 + c_y^2 \leqslant \tfrac{1}{2}. \tag{44}$$

This result may also be derived from (30).

Surprisingly enough, inequality (44), along with (27), is also a sufficient stability condition! To prove this statement, the graphical interpretation used so far is replaced by another method:

First, we define

$$c_x^2 + c_y^2 = \tfrac{1}{2}(1-\varepsilon), \tag{45}$$

$$\frac{c_x^2}{c_x^2 + c_y^2} = \mu, \qquad 0 \leqslant \mu \leqslant 1 \tag{46}$$

$$U = \cos^2 \theta_x, \qquad 0 \leqslant U \leqslant 1 \tag{47}$$

$$V = \cos^2 \theta_y, \qquad 0 \leqslant V \leqslant 1. \tag{48}$$

Next, we write b in terms of the above variables,

$$b = -1 + 2(b_0 + b_1 \varepsilon + b_2 \varepsilon^2), \tag{49}$$

where

$$b_0 = -\phi^2 UV[\mu + (1-\mu)V][(1-\mu)+\mu U] + UV[\mu\sqrt{U/V} + (1-\mu)\sqrt{V/U}]^2, \quad (50)$$

$$b_1 = -\phi^2 UV[\mu(1-U) + (1-\mu)(1-V) - 2\mu(1-\mu)(1-U)(1-V)] + 2UV\left[\frac{\mu}{V} + \frac{1-\mu}{U}\right][\mu(1-U) + (1-\mu)(1-V)], \quad (51)$$

$$b_2 = -\phi^2 UV(1-U)(1-V)\,\mu(1-\mu) + (1-U)(1-V) \times [\mu\sqrt{(1-U)/(1-V)} + (1-\mu)\sqrt{(1-V)/(1-U)}]^2. \quad (52)$$

Finally, we show that

$$b_0 \geqslant 0, \qquad b_1 \geqslant 0, \qquad b_2 \geqslant 0, \quad (53)$$

provided $\phi^2 \leqslant 1$.

To do so, it is useful to note that

$$\frac{\mu}{V} + \frac{1-\mu}{U} \geqslant 1, \quad (54)$$

$$-\mu(1-U) + (1-\mu)(1-V) + 2\mu(1-\mu)(1-U)(1-V) \geqslant -\mu(1-U) + (1-\mu)(1-V), \quad (55)$$

$$\mu\sqrt{(1-U)/(1-V)} + (1-\mu)\sqrt{(1-V)/(1-U)} \geqslant 2\sqrt{\mu(1-\mu)}. \quad (56)$$

By introducing (54) and (55) into (51), bearing in mind that $\phi^2 \leqslant 1$, it is seen that $b_1 \geqslant 0$. Similarly, inequalities (27) and (56) imply that $b_2 \geqslant 0$. Turning now to b_0, it is sufficient to show that

$$[\mu + (1-\mu)V][(1-\mu)+\mu U] \leqslant [\mu\sqrt{U/V} + (1-\mu)\sqrt{V/U}]^2 \quad (57)$$

or, equivalently,

$$a(U, V) = \left[\mu^2\frac{U}{V} + 2\mu(1-\mu) + (1-\mu)^2\frac{V}{U}\right] - [\mu + (1-\mu)V][(1-\mu)+\mu U] \geqslant 0. \quad (58)$$

The location of the minimum of $a(U, V)$ satisfies

$$\frac{\partial a}{\partial U} = \frac{\mu^2}{V} - (1-\mu)^2\frac{V}{U^2} - \mu[\mu + (1-\mu)V] = 0$$
$$\frac{\partial a}{\partial V} = -\mu^2\frac{U}{V^2} + \frac{(1-\mu)^2}{U} - (1-\mu)[(1-\mu)+\mu U] = 0, \quad (59)$$

implying

$$\mu^2 U + 2\mu(1-\mu)\,UV + (1-\mu)^2\,V = 0, \quad (60)$$

which cannot be verified in the interior of the domain of definition. Thus, the local extrema may be found only on the boundary of the domain defined by (47), (48). For symmetry reasons, we will analyse only the case $U = 0$ or $U = 1$. For $U = 0$, (58) is obviously satisfied. For $U = 1$ we have

$$a(1, V) = \frac{\mu}{V}[\mu(1-V)^2 + V(1-V)] \geqslant 0 \quad (61)$$

and, thus, $b_0 \geqslant 0$.

From (49) and (53) it is thus seen that $b \geqslant -1$ and that the maximum of b corresponds to $\varepsilon = 1$. In this case $b = 1 - 2\phi^2 UV \leqslant 1$ and condition (22) holds true.

5.4. *D-Grid*

In Table I, one may see that, from the features of the $b = -1$ ellipse, ξ_x and ξ_y depend upon α. For a particular value of α, (ξ_x, ξ_y) describes a hyperbola, the equation of which reads

$$(c_x^2\alpha^2 - \xi_x)(c_y^2\alpha^2 - \xi_y) = c_x^2 c_y^2\alpha^6. \quad (62)$$

To ensure numerical stability, one must prevent the above hyperbola from penetrating into the A_- region (Fig. 5). Here, only the case $c_x = c = c_y$ is thoroughly examined. Accordingly, the $\xi_x = \xi_y$ line is a symmetry axis for both the ellipses (26) and hyperbolas (62). In order to avoid having the hyperbolas enter into the A_- zone, we must ensure that the $b = -1$ ellipse and the hyperbola corresponding to a given value of α have, at most, a tangency point; this tangency point inevitably is on the symmetry axis. The intersection of the hyperbola with the symmetry axis is at

$$\xi_x = \xi_y = \alpha^2 c^2(1-\alpha). \quad (63)$$

Thus, the stability condition is

$$\alpha^2 c^2(1-\alpha) \leqslant \xi_{=,-} = \frac{1}{2}\frac{(1-\alpha\,|\phi|)}{(2-\alpha\,|\phi|)} \quad (64)$$

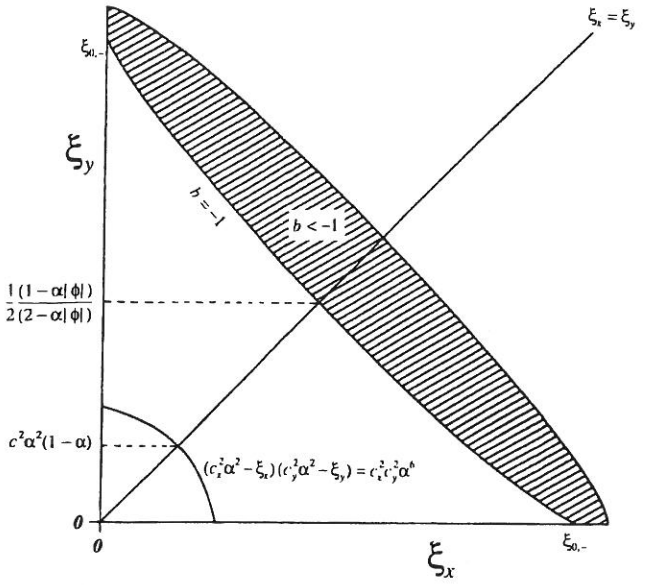

FIG. 5. Stability condition for grid D with $c_x = c = c_y$.

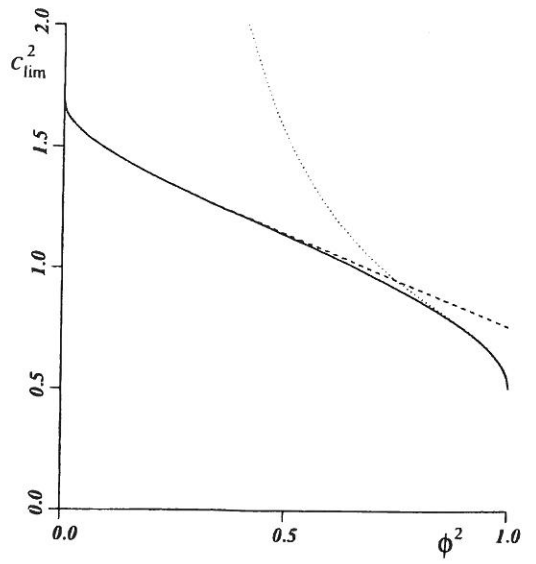

FIG. 6. Isotropic stability condition $c^2_{\text{lim}}(\phi^2)$ for grid D (dashed and dotted lines are the asymptotic expansions).

or

$$c^2 \leqslant c^2_{\text{lim}} = \frac{1}{2} \min_{0 \leqslant \alpha \leqslant 1} \left[\frac{1 - \alpha\,|\phi|}{\alpha^2(1-\alpha)(2-\alpha\,|\phi|)} \right], \tag{65}$$

which is plotted in Fig. 6. The upper limit c^2_{lim} admits the following asymptotic expansions:

$$c^2_{\text{lim}} = \tfrac{27}{16} - \tfrac{9}{16}\,|\phi| - \tfrac{13}{64}\,\phi^2 - \tfrac{19}{216}\,|\phi|^3 - \tfrac{31}{648}\,\phi^4 + O(\phi^5), \quad |\phi| \ll 1, \tag{66}$$

$$c^2_{\text{lim}} = \tfrac{1}{2} + \psi + \tfrac{1}{2}\psi^2 - \tfrac{1}{2}\psi^3 + \psi^4 - \tfrac{37}{8}\psi^5 + 22\psi^6 + O(\psi^7), \quad \psi = \sqrt{1 - |\phi|} \ll 1. \tag{67}$$

If $\phi^2 = 1$, the necessary and sufficient stability condition (Appendix II) is

$$c_x^2,\, c_y^2 \leqslant \tfrac{1}{2}, \tag{68}$$

which matches (67) when $c_x = c = c_y$.

Finally, for $c_y = 0$,

$$c_x^2 \leqslant \tfrac{1}{2}(1 + \sqrt{1 - \phi^2})^2 \tag{69}$$

is the necessary and sufficient stability condition, consistent with (68) and (30).

It is worth pointing out an important difference between the A and B grids, on the one hand, and the C and D grids, on the other hand. When $\phi^2 = 1$, numerical stability requires $c_x = 0 = c_y$ for the former, while c_x, c_y may be nonzero for the latter. This discrepancy stems from the four-points averaging of the velocity that one performs in the expression of the Coriolis force on the C and D grids.

6. DISCUSSION

In many descriptions of geophysical fluid models, it is stated that the stability condition of the complete numerical scheme is roughly given by that of the pure gravity waves propagation. We have shown that, at least for a simple FBTCS discretization, this view is not correct.

Many geophysical fluid models allow the propagation of inertia-gravity waves. The FBTCS discretization is very popular. One may thus wonder why the inadequacy of the pure gravity waves stability criterion has not been extensively reported so far. Three basic reasons may be put forward.

First, it is customary to apply a "security factor" on the maximum allowable time step derived from a simple stability criterion. As a consequence one may choose a time step that, by chance, satisfies the more restrictive stability requirement for the propagation of inertia-gravity waves.

Second, analytical and numerical calculations show that the most unstable modes are short wavelength modes, but not the $2\Delta x$ mode. The dissipation present in most models is generally of Laplacian or bi-Laplacian type, which means that the damping is more important on the short wavelength modes. It is thus possible that the dissipation term counterbalances the destabilizing effect of the Coriolis force.

Finally, one must bear in mind that, because of the

discrete nature of the numerical scheme, not all the wavelengths are permitted. Equivalently, one may not consider that all θ_x, θ_y correspond to modes actually allowed by the grid. Indeed, numerical calculations show that the instability domain consists of narrow bands in the θ_x, θ_y space. The probability that a given grid does not represent the unstable modes is thus not negligible, so avoiding the occurrence of the instability. In (c_x, c_y) space, for a given ϕ, depending on the number of grid points and thus on the discrete values of θ_x, θ_y represented by the grid, there are indeed stability regions, where normally the scheme should be unstable. This is due to the fact that the actual grid does not resolve these unstable modes. Only when the number of grid points increases, these stability regions disappear and the analytical stability condition is verified everywhere.

APPENDIX I: PURE GRAVITY WAVE STABILITY CONDITION FOR THE D GRID

The stability condition is $\xi \leqslant \xi_* = 1$, but one has to translate this condition into conditions on c_x, c_y, and ϕ. To do this, we have to calculate the maximum of $\xi(\theta_x, \theta_y)$. The extrema are found for

$$\begin{aligned}\frac{\partial \xi}{\partial \theta_x} &= 2\cos\theta_x \sin\theta_x \cos^2\theta_y \\ &\quad \times \{c_x^2 - 2c_x^2 \sin^2\theta_x - c_y^2 \sin^2\theta_y\} = 0 \\ \frac{\partial \xi}{\partial \theta_y} &= 2\cos\theta_y \sin\theta_y \cos^2\theta_x \\ &\quad \times \{c_y^2 - 2c_y^2 \sin^2\theta_y - c_x^2 \sin^2\theta_x\} = 0.\end{aligned} \tag{A.1}$$

It is immediately seen that $\theta_x = \pi/2$ or $\theta_y = \pi/2$ correspond to the minima of ξ. Local maxima are at

$$\sin^2\theta_x = 0, \quad \sin^2\theta_y = \tfrac{1}{2}, \quad \rightarrow \xi = \tfrac{1}{4}c_y^2, \tag{A.2}$$

$$\sin^2\theta_x = \tfrac{1}{2}, \quad \sin^2\theta_y = 0, \quad \rightarrow \xi = \tfrac{1}{4}c_x^2, \tag{A.3}$$

$$\sin^2\theta_x = \frac{2c_x^2 - c_y^2}{3c_x^2}, \quad \sin^2\theta_y = \frac{2c_y^2 - c_x^2}{3c_y^2}, \quad \rightarrow \xi = \frac{(c_x^2 + c_y^2)^3}{c_x^2 c_y^2}. \tag{A.4}$$

The $\xi \leqslant 1$ condition is thus satisfied if and only if

$$\begin{aligned} &c_x^2 \leqslant 4, \\ &c_y^2 \leqslant 4, \\ &\frac{(c_x^2 + c_y^2)^3}{c_x^2 c_y^2} \leqslant 27 \qquad \text{if} \quad c_x^2 \leqslant 2c_y^2 \leqslant 4c_x^2 \end{aligned} \tag{A.5}$$

because the latter condition applies only if the roots found for $\sin^2\theta_x$ and $\sin^2\theta_y$ in (A.4) are positive.

APPENDIX II: NECESSARY AND SUFFICIENT STABILITY CONDITION FOR THE D GRID WITH $\phi^2 = 1$

When $\phi^2 = 1$, the numerical scheme is stable if and only if $c_x^2 \leqslant \frac{1}{2}$, $c_y^2 \leqslant \frac{1}{2}$. The demonstration is outlined. We define

$$c_x^2 = \tfrac{1}{2}(1 - \varepsilon_x), \tag{A.6}$$

$$c_y^2 = \tfrac{1}{2}(1 - \varepsilon_y), \tag{A.7}$$

and we rewrite b as

$$\begin{aligned} b = -1 + 2[&b_0 + b_{1\varepsilon_x}\varepsilon_x + b_{1\varepsilon_y}\varepsilon_y \\ &+ b_{2\varepsilon_x}\varepsilon_x^2 + b_{2\varepsilon_y}\varepsilon_y^2 + b_{\varepsilon_x\varepsilon_y}\varepsilon_x\varepsilon_y], \end{aligned} \tag{A.8}$$

where

$$\begin{aligned} b_0 = &-\cos^6\theta_x \cos^6\theta_y \sin^2\theta_x \sin^2\theta_y \\ &+ \cos^4\theta_x \cos^4\theta_y (\sin^2\theta_x + \sin^2\theta_y) \\ &\times (1 + \sin^2\theta_x + \sin^2\theta_y) - \cos^2\theta_x \cos^2\theta_y \\ &\times (1 + 2\sin^2\theta_x + 2\sin^2\theta_y) + 1, \end{aligned} \tag{A.9}$$

$$\begin{aligned} b_{1\varepsilon_x} = &\cos^2\theta_x \cos^2\theta_y \sin^2\theta_x [2 + \cos^4\theta_x \cos^4\theta_y \sin^2\theta_y \\ &- 2\cos^2\theta_x \cos^2\theta_y (\sin^2\theta_x + \sin^2\theta_y) \\ &- \cos^2\theta_x \cos^2\theta_y], \end{aligned} \tag{A.10}$$

$$\begin{aligned} b_{1\varepsilon_y} = &\cos^2\theta_x \cos^2\theta_y \sin^2\theta_y [2 + \cos^4\theta_x \cos^4\theta_y \sin^2\theta_x \\ &- 2\cos\theta_x \cos^2\theta_y (\sin^2\theta_x + \sin^2\theta_y) \\ &- \cos^2\theta_x \cos^2\theta_y], \end{aligned} \tag{A.11}$$

$$b_{2\varepsilon_x} = \cos^4\theta_x \cos^4\theta_y \sin^4\theta_x, \tag{A.12}$$

$$b_{2\varepsilon_y} = \cos^4\theta_x \cos^4\theta_y \sin^4\theta_y, \tag{A.13}$$

$$b_{\varepsilon_x\varepsilon_y} = \cos^4\theta_x \cos^4\theta_y \sin^2\theta_x \sin^2\theta_y (2 - \cos^2\theta_x \cos^2\theta_y). \tag{A.14}$$

One may show that

$$\begin{aligned} &b_0 \geqslant 0, \quad b_{\varepsilon_x\varepsilon_y} \geqslant 0, \quad b_{2\varepsilon_x} \geqslant 0, \\ &b_{2\varepsilon_y} \geqslant 0, \quad b_{1\varepsilon_x} \geqslant 0, \quad b_{1\varepsilon_y} \geqslant 0, \end{aligned} \tag{A.15}$$

wich implies that $b \geqslant 1$ when $\varepsilon_x \geqslant 0$, $\varepsilon_y \geqslant 0$. Furthermore, when $(\varepsilon_x, \varepsilon_y) = (1, 1)$, we recover the pure inertia wave scheme, where we have already demonstrated that $b \leqslant 1$. Inequality (68) is thus the stability condition for $\phi^2 = 1$.

ACKNOWLEDGMENTS

Part of the present work has been done when the authors were Research Assistants at the National Fund for Scientific Research of Belgium. This